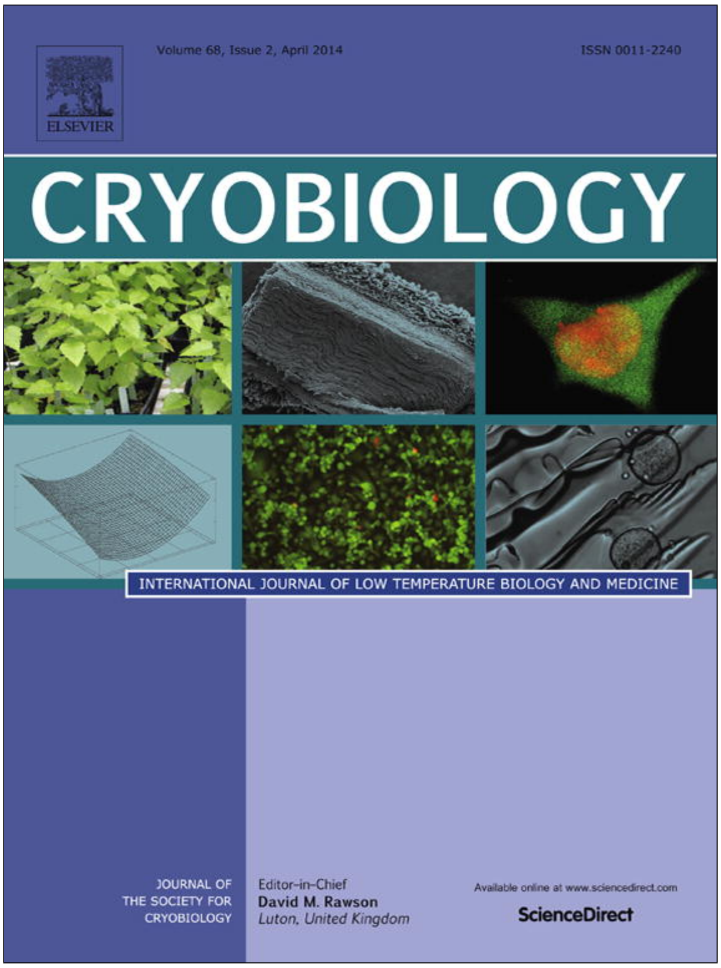
Volume 68, Issue 2, April 2014
ISSN 0011-2240
ELSEVIER
CRYOBIOLOGY
INTERNATIONAL JOURNAL OF LOW TEMPERATURE BIOLOGY AND MEDICINE
JOURNAL OF THE SOCIETY FOR CRYOBIOLOGY
Editor-in-Chief
David M. Rawson
Luton, United Kingdom
Available online at www.sciencedirect.com
ScienceDirect

Cryobiology 68 (2014) 194–199

Contents lists available at ScienceDirect

Cryobiology

journal homepage: www.elsevier.com/locate/ycryo

Comparison of percutaneous cryoablation with microwave ablation in a porcine liver model ☆

Lizhi Niu [a,b,1], Jialiang Li [a,1], Jianying Zeng [a,1], Liang Zhou [a], Song Wang [c], Xulong Zhou [a], Lin Sheng [c,*], Jibing Chen [b,*], Kecheng Xu [a,b]

[a] Fuda Cancer Hospital, School of Medicine, Jinan University, No. 2 of Tangdexi Road, Tianhe District, Guangzhou, Guangdong 510665, China
[b] Fuda Institute of Cryosurgery for Cancer, No. 2 of Tangdexi Road, Tianhe District, Guangzhou 510665, China
[c] Department of Interventional Ultrasound, Yuquan Hospital, Tsinghua University, No. 5 of Shijingshan Road, Shijingshan District, Beijing 100049, China

ARTICLE INFO

Article history:
Received 17 June 2013
Accepted 13 January 2014
Available online 29 January 2014

Keywords:
Cryoablation
Microwave ablation
Porcine model
Liver model

ABSTRACT

We compared imaging and pathological changes between argon–helium cryosurgical (AH) and microwave (MW) ablation in a porcine liver model. Immediately after ablation, computed tomography (CT) imaging showed that the area affected by MW ablation was considerably greater than that affected by AH ablation; moreover, the surface area of necrotic tissue was considerably greater in the AH group, whereas the depth of the necrotic area was similar. Seven days after ablation, the affected area had not changed much in the AH group, but it had significantly increased in the MW group; similarly, the surface and depth of the necrotic areas had not changed much in the AH group, but they had increased significantly in the MW group. The pathological findings showed similar definitive areas for both groups at both time points. The findings indicated that long time after both therapies, complete tissue necrosis can be achieved, but the extent and depth of necrosis differ: necrosis foci after AH ablation could be predicted by ice ball under CT image, and necrosis foci after MW ablation will increase obviously. MW ablation might therefore be suitable for tumors with a larger volume and simple anatomical structures, and AH ablation might be suitable for tumors with complex anatomical structures or those located near important organs. These two methods could therefore be used in combination in clinical settings, but details of the procedure need to be studied.

Introduction

Hepatocellular carcinoma (HCC) is the fifth most common cancer worldwide [23]. Unfortunately, a large proportion of HCC patients do not meet the criteria for tumor resection because of factors such as poor hepatic reserve (cirrhosis), multicentric tumors and extrahepatic disease [5,10]. An alternative to resection is direct ablative treatment, which includes radiofrequency ablation and cryotherapy. With advances in imaging technology and improvements in ablation instruments, the clinical application of in situ cancer ablation methods has gradually expanded, with argon-helium cryosurgical (AH) and microwave (MW) ablation now providing all the benefits of radiofrequency and the liquid nitrogen cryosurgical system, and also demonstrating substantial advantages [8,20,26]. Both the AH and MW ablation techniques are associated with higher intratumoral temperatures, larger tumor ablation volumes, faster ablation times, simultaneous use of multiple probes [14,33], optimal heating of cystic masses and tumors close to the vessels, and less procedural pain [14,25,26,33]. Over the years, trials on cancers of the liver [26,34], lung [31,38], kidney [13,32], bone [26,29] and pancreas [15,36] have demonstrated good treatment outcomes with these two ablation methods.

In the past, on the characteristics of two ablation methods had been set forth by a lot of researches, respectively. Ablation with MW treatment is mainly performed using a thermal field greater than 60 °C that covers the tumor, and contrast-enhanced sonography or computed tomography (CT) is usually required to observe the ablation foci [3,4,21]. On the other hand, AH treatment is mainly conducted using a thermal field less than −20 °C that covers the tumor, and conventional sonography or CT can easily depict the ablation foci [2]. So maybe there are a litter difference for protocols between centers, the freeze–thaw cycle of AH ablation is mostly two, the time for MW ablation is mostly one, power is mostly 100%, time length are all stricted by iceball size and thermal field. But in clinical treatment, indications of the two methods are still confused. The aim of this study was to

☆ *Statement of funding:* This work was supported by a Grant from the Innovation Fund of the Ministry of Science and Technology, China (No. 09C26221102792).
* Corresponding authors. Fax: +86 (020) 38993994x8700.
E-mail addresses: fudaclab@gmail.com (L. Sheng), fudaclab@gmail.com (J. Chen).
[1] These three authors contributed equally to this work and share first authorship.

http://dx.doi.org/10.1016/j.cryobiol.2014.01.005
0011-2240/

compare these two minimally invasive ablation methods, in terms of thermal field, imaging, and pathological changes over time, as well as the characteristics of tissues in which necrosis was induced. This work will provide the basis for selecting ablative methods according to the characteristics of tumor.

Materials and methods

Animals

Twelve certified healthy miniature Tibetan pigs that weighed between 27 and 32 kg were provided by the Animal Experimental Center of South Medical University (Guangzhou, China). Approval for the study was obtained from the Research Animal Care and Use Committee of our hospital, and all husbandry and experimental studies complied with the National Research Council's Guide for the Care and Use of Laboratory Animals.

Ablation procedures

All procedures were performed under general anesthesia. Each pig was placed in the left decubitus position. Then, an intramuscular injection of ketamine hydrochloride, promethazine hydrochloride and atropine was given to induce general anesthesia, and the anesthesia was maintained using isoflurane (1.5%) and oxygen (3 L/min) administered through a mask. Using a sterile technique, the AH or MW probes were inserted percutaneously under the guidance of double-row CT (Somatom Emotion, Siemens; pitch, 1; slice thickness and distance, 2 mm; current, 174.0 mA; voltage, 130.0 kV). The probes were both inserted approximately 4.5 cm into the same right middle lobe from the left lying position, between the 11th and 12th ribs. Vital organs, such as the lung, the gall bladder and the stomach, need to be avoided during ablation, so the ablation points were approximately 5 cm apart. Four 14.5-gauge thermal probes (iron-copper thermocouple wire, Omega Engineering Inc., Stamford, CT) were also positioned in the liver lobe, 5, 10, 15 and 20 mm from the ablation probe, in accordance with the commonly used temperature measurement method for MW [6] and AH [9]. Instruments, protocols, visualized monitoring, temperature test and analysis were listed as Table 1.

Six pigs were returned to their cages and given regular food for 7 days. The other six pigs were sacrificed immediately after the operation, and liver samples were stained with hematoxylin and eosin and subjected to pathological analysis. 5-μm thick slices were made, and pathological analysis was performed for overall and local characteristics. The typical sampling sites of the two groups were the widest section of the lesion and the section at a right angle to the angle of needle insertion.

Statistical analysis

All analyses were performed using the Graphpad Prism (GraphPad Inc., CA) software. All data are expressed as the mean ± standard deviation. Low-density shadow after CT test and complete necrotic region after pathologic test were compared using the *t*-test. $P < 0.05$ was considered to indicate statistical significance, with $P < 0.01$ and $P < 0.001$ indicating highly significant differences.

Results

CT findings

In the pigs that were sacrificed and examined on the same day of the operation, areas showing freezing injury and/or iceballs were seen to form rapidly under CT guidance. Immediately after the second AH freezing processes (Fig. 1A1), the low-density shadows on conventional CT scans were (2.8 ± 0.1 cm) × (3.9 ± 0.4 cm) (middle two shadows in the image) in size. The results from the second freezing fitted perfectly with the results of the enhanced CT images, that is, (2.6 ± 0.1 cm) × (3.3 ± 0.4 cm) (right).

Immediately after MW ablation (Fig. 1A2), the diameter of the thermolesion on a conventional CT scan was measured, but the imaging observations were unclear (middle). Contrast-enhanced CT showed that the area of the thermolesion was (3.3 ± 0.2 cm) × (3.4 ± 0.3 cm) (right). 7 days later, the corresponding low-density shadows with AH ablation were (2.7 ± 0.2 cm) × (3.4 ± 0.8 cm), which were similar to those observed on the operation day ($P > 0.05$, figures not shown); with MW ablation, the low-density shadows were (4.2 ± 0.3 cm) × (3.4 ± 0.4 cm), which showed a clear increase from the operation day ($P < 0.05$, figures not shown).

Changes in thermal field and characteristics of ablated tissue and lesions

Data on temperature changes after AH and MW ablation were analyzed using a multi-function data collector (Fig. 1(B1 and B2)), which showed the typical temperature changes following AH and MW ablation, respectively. Observation of the vertical section along the route of the needle showed that necrotic regions of both groups were in a gyro shape. In the case of AH ablation (Fig. 1C1), the surface and inner lesions were purple in color, and the surface and depth of the necrotic region were 2.85 ± 0.4 and 2.89 ± 0.5 cm, respectively. In the case of MW ablation (Fig. 1C2), the surface and inner lesions were white and brown in color, respectively, and the surface and depth of the necrotic region were 2.83 ± 0.5 and 3.75 ± 0.4 cm, respectively. 7 days later, the surface and inner lesions of AH ablation were both purple in color, and the surface and depth of the necrotic region were 2.3 ± 0.5 and 2.9 ± 0.3 cm, respectively, similar to the values observed on the operation day. With MW ablation, the surface and inner lesions were both brown in color, and the surface and depth of the necrotic region were 2.83 ± 0.5 and 4.4 ± 0.4 cm, respectively; the necrotic region was therefore much larger than that observed on the operation day.

Table 1
Instruments, protocols, visulized monitoring, temperature test and analysis.

	Instrument	Protocol	Visualized monitoring	Temperature test	Temperature analysis
AH Ablation	Cryo-Hit™ Cryosurgical System (Galil, Israel), cryoprobes (diameter, 1.47 mm)	Output power 100%, freeze (10 min)-thaw (3 min), 2 cycles	Iceballs and cryolesions were measured by conventional CT	16-channel multi-function data collector (34970A, Agilent Co, Palo Alto, CA.; scan rate, 250 channels/s)	Agilent BenehLink Data Logger software
MW Ablation	UMC-I type (Aerospace Industry Ministry, China), radiating segment 11 mm in length	Output power 60 W, a single "10 min" cycle	Thermolesions were measured by conventional and enhanced CT		

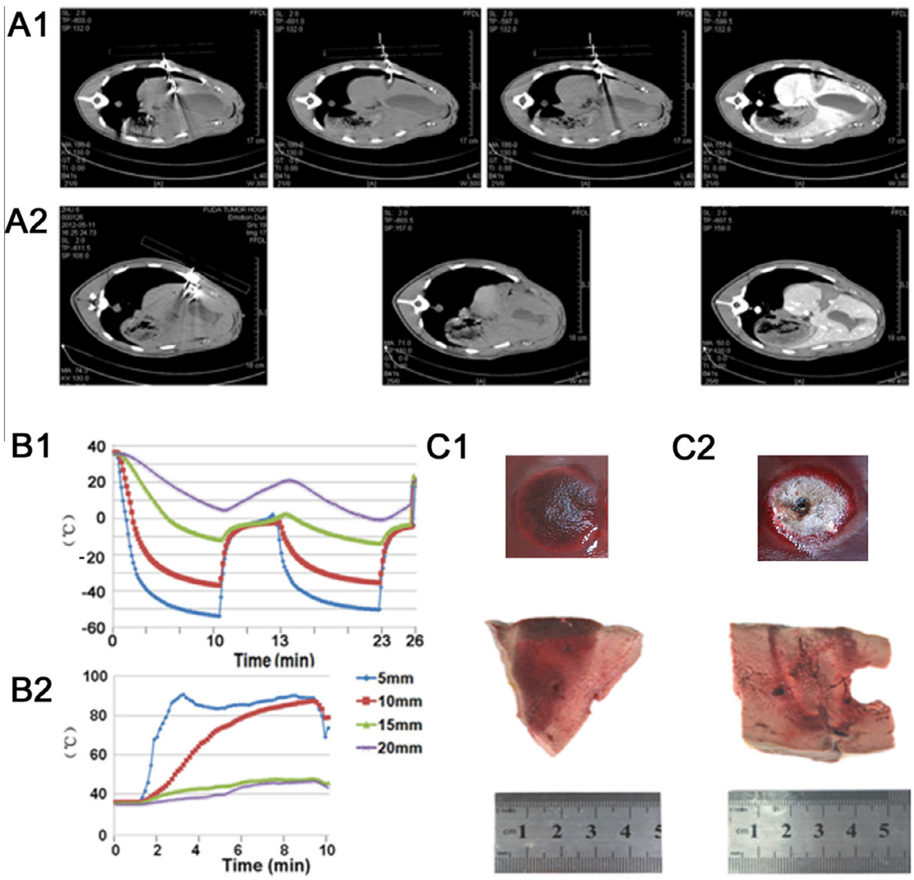

Fig. 1. Comparison of biological outcomes during and after AH and MW ablation on the same day of the procedure. Six pigs underwent AH and MW ablation successively. (A1/2) typical imaging findings for AH and MW ablation, respectively; (B1/2) typical temperature changes following AH and MW ablation, respectively; (C1/2) typical lesion presentation after AH and MW ablation, respectively: upper image, external surface; lower image, section along the route of the needle.

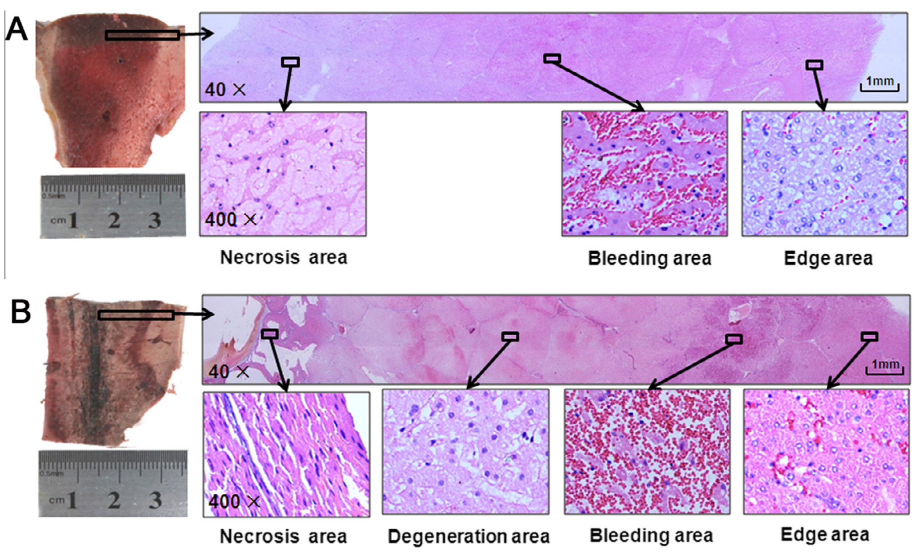

Fig. 2. Pathological examination of hepatic damage immediately after ablation. Four to six sections were examined for each sample, and six samples for each group. (A) Typical findings for AH ablation, including three definitive areas; (B) typical findings for MW ablation, including four definitive areas.

Pathological changes in ablated tissue

The typical changes immediately after AH ablation covered three definitive areas (Fig. 2A). In coagulative necrosis area, the liver cable and liver plate had a net-like structure; widespread nuclear pyknosis and a small amount of fragmentation. In bleeding area, significant hemorrhage in the liver sinusoidal areas. The surface and depth of the necrotic areas were 1.6 ± 0.2 and 2.8 ± 0.3 cm, respectively. In the case of MW ablation (Fig. 2B), we found an additional "degeneration area" which was characterized by an increased volume of hepatocytes with unclear boundaries, marked edema, and thick red-staining particles in the cytoplasm. The

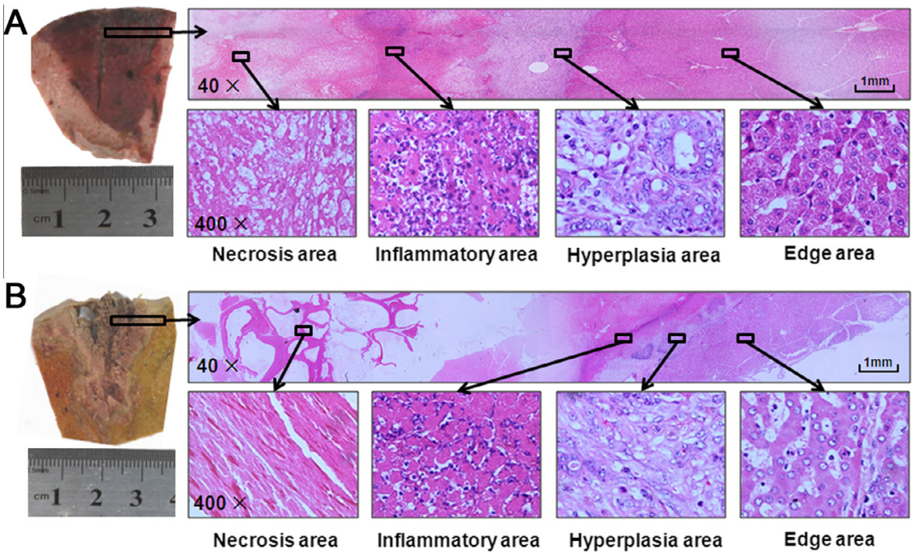

Fig. 3. Pathological examination of hepatic damage 7 days after ablation. Four to six sections were examined for each sample and six samples for each group. (A) and (B) represent typical findings for the AH and MW groups, respectively, both panels including four similarly definitive areas.

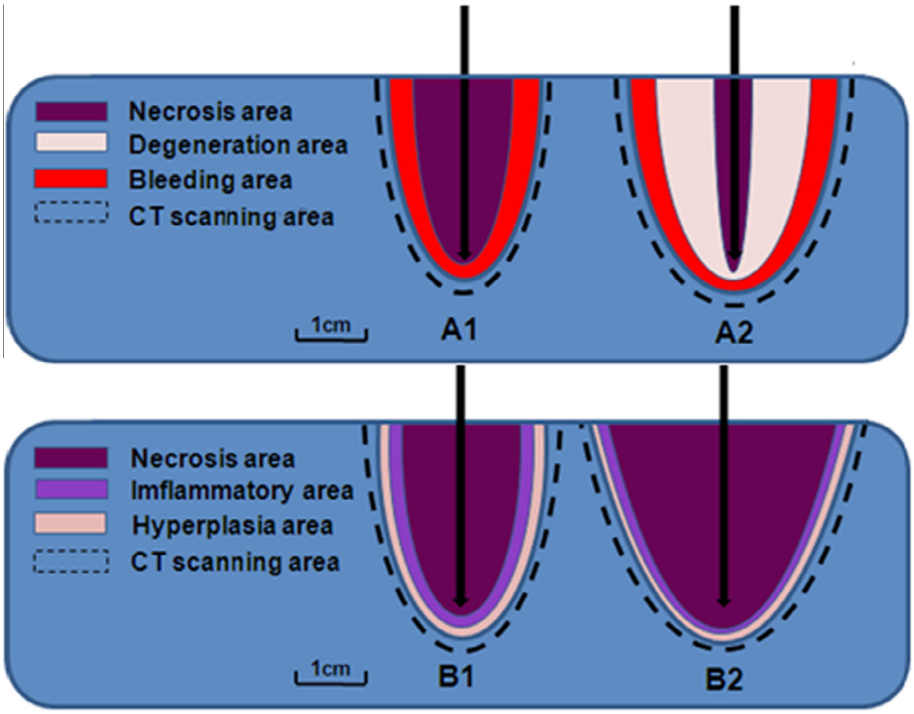

Fig. 4. Schematic representation of the pathological regions in the cryolesions and thermolesions. The blue background represents hepatic parenchyma, and the black arrows in the necrotic area represent the ablation probes. A1 and A2 depict typical cryolesions and thermolesions, respectively, immediately after ablation. B1 and B2 represent typical cryolesions and thermolesions, respectively, 7 days after ablation. (For interpretation of the references to color in this figure legend, the reader is referred to the web version of this article.)

surface and depth of the necrotic areas (complete necrosis regions) were 0.4 ± 0.4 and 2.9 ± 0.6 cm, respectively. In different sections, each area was at a different distance from the route of the needle.

7 days after ablation, the "necrosis area," the "inflammatory infiltrate area," the "hyperplasia area" and the "edge area" (Fig. 3) were found in cryozone. In necrosis area, extensive coagulative necrosis was found with incomplete tissue structure; liver cable had disintegrated to a structure similar to a net; liver sinusoidal dilatation was present with shrinking hepatocytes, a cytoplasmic pool, and homogenization. Then extensive infiltration of inflammatory cells and significant hyperplasia of granulation tissue were found, gradually transfer to normal tissue. The surface and depth of the necrotic area (only inclusive of complete necrotic regions) were 1.8 ± 0.3 and 2.83 ± 0.6 cm, respectively for AH ablation, and 3.18 ± 0.7 and 3.0 ± 0.4 cm, respectively for MW ablation; with both treatments, the values were obviously greater than those observed immediately following ablation ($P < 0.05$ for all).

Discussion

We have satisfactorily compared the biological outcomes of AH and MW ablation in a porcine liver model, including changes in the thermal field, and in imaging and pathological features over time.

In accordance with the findings of commonly used ablation protocols, flake necrosis and hemorrhage appeared immediately after two cycles of AH ablation [7,19,30]. However, a larger degeneration area and a small amount of necrosis and hemorrhage were observed immediately after MW ablation. With time, the degeneration and bleeding areas gradually evolved into the necrotic area, which implies that degeneration and bleeding areas observed immediately after ablation can be viewed as the incipient complete necrotic area (Fig. 4).

One of the main differences in pathological change 7 days after AH ablation and MW ablation is the inflammation area. That is, AH ablation can induce a much greater inflammation area than MW ablation. These results are similar to those of Ng et al. [17]. They proved that hepatic cryoablation in porcine liver can cause more severe systemic inflammation than hepatic radiofrequency ablation or resection. Two phenomena are associated with systemic inflammation in hepatic cryoablation, one of which is the cryoshock after hepatic cryoablation. It is a rare fatal complication [35] caused by the release of intracellular cytotoxic substances during the freeze/thaw process of hepatic cryotherapy [17]. The second is cryoimmune response, which may be induced by the release of intracellular antigens against cryoablation and be accompanied by inflammatory cell infiltration [18]. Compared with AH ablation, MW ablation has been associated with a significant decrease in cytokine response [1]. Since inflammation response in tumor ablation sites is a key factor that influences cancer development [16], further investigation should be conducted to compare the inflammation response between AH ablation and MW ablation.

In order to increase the safety of ablation, accurate tumor ablation under CT guidance is crucial. The main purpose of tumor ablation is complete tumor tissue necrosis, and pathological changes are the most accurate indicator of the extent of tissue damage. Moreover, imaging cannot adequately depict treatment-related swelling [24], and the subsequent damages of ablation are observed 4–7 days after the procedure [8,17]. This paper therefore also investigated the relationship between imaging findings and pathological necrosis on the day of ablation and 7 days after ablation. The complete area of necrosis induced by AH ablation did not show a remarkable change after 7 days, and the range of the final necrotic foci could be predicted by the size of the ice ball on CT images. On the other hand, with MW ablation, the area of complete necrosis had clearly enlarged by the 7th day, with an obvious increase in necrotic foci on contrast-enhanced CT images. This may increase the risk of complications, especially for tumors near large vessels, the bowel, diaphragm and bile ducts.

In terms of safety, although AH ablation had a longer operation time, ice ball formation could be observed at any point of time and CT imaging reflected well the ice ball formation and tissue necrosis. This precise ablation can be beneficial for preservation of liver function in patients with relatively poor liver function [11]. At the same time, compared with MW ablation, the necrosis area in the case of AH ablation is quite small. In the case of large or irregularly shaped tumors, AH ablation may increase the chance of tumor recurrence, so two or three probes can be combined to make a larger ice ball or combined with iodine-125 seeds [36,37]. In the case of MW ablation, the necrosis range is relative large and the real necrosis range may exceed the boundary of CT imaging 7 days after ablation. Therefore, this method might be particularly suitable for the ablation of tumors with a larger volume and simple anatomical structures, such as the central portion of the liver.

In summary, our preliminary results show that MW ablation can result in a larger necrosis than AH ablation. Moreover, with AH ablation, the inflammation is pathologically detectable and CT imaging can reflect ice ball formation and tissue necrosis better than with MW ablation. These findings suggest that both treatments may complement each other clinically. MW ablation might be particularly suitable for the ablation of tumors with a larger volume and simple anatomical structures and AH ablation may be suitable for tumors located near large vessels, the bowel, diaphragm and bile ducts. In fact, it is difficult to choose a suitable technique for liver ablation because many more factors need to be considered, such as the minimal heat sink protective effect of large vessels (diameter > 3 mm) [27,28], prevention and treatment of possible deadly complications such as intestinal and biliary duct injury by warm water perfusion [12], economic well-being of the patient, and the induction of cryoimmunity in some patients [22]. Therefore, much more work needs to be done to compare these two techniques in the clinical setting and establish an efficient ablation protocol.

References

[1] F. Ahmad, G. Gravante, N. Bhardwaj, A. Strickland, R. Basit, K. West, R. Sorge, A.R. Dennison, D.M. Lloyd, Changes in interleukin-1beta and 6 after hepatic microwave tissue ablation compared with radiofrequency, cryotherapy and surgical resections, Am. J. Surg. 200 (2010) 500–506.
[2] T.D. Atwell, M.A. Farrell, M.R. Callstrom, J.W. Charboneau, B.C. Leibovich, D.E. Patterson, G.K. Chow, M.L. Blute, Percutaneous cryoablation of 40 solid renal tumors with US guidance and CT monitoring: initial experience, Radiology 243 (2007) 276–283.
[3] G. Carrafiello, D. Lagana, M. Mangini, F. Fontana, G. Dionigi, L. Boni, F. Rovera, S. Cuffari, C. Fugazzola, Microwave tumors ablation: principles, clinical applications and review of preliminary experiences, Int. J. Surg. 6 (Suppl 1) (2008) S65–69.
[4] L. Chami, N. Lassau, D. Malka, M. Ducreux, S. Bidault, A. Roche, D. Elias, Benefits of contrast-enhanced sonography for the detection of liver lesions: comparison with histologic findings, Am. J. Roentgenol. 190 (2008) 683–690.
[5] G.M. Dusheiko, K.E. Hobbs, R. Dick, A.K. Burroughs, Treatment of small hepatocellular carcinomas, Lancet 340 (1992) 285–288.
[6] W. Fan, X. Li, L. Zhang, H. Jiang, J. Zhang, Comparison of microwave ablation and multipolar radiofrequency ablation in vivo using two internally cooled probes, Am. J. Roentgenol. 198 (2012) W46–W50.
[7] K. Hashimoto, Y. Izumi, Y. Yamauchi, H. Yashiro, M. Inoue, S. Nakatsuka, H. Nomori, Prediction of the critical thermal zone during pulmonary cryoablation on computed tomography from correlated experimental and clinical findings, Thorac. Cardiovasc. Surg. 145 (2013) 832–838.
[8] P.M. Hewitt, J. Zhao, J. Akhter, D.L. Morris, A comparative laboratory study of liquid nitrogen and argon gas cryosurgery systems, Cryobiology 35 (1997) 303–308.
[9] J.L. Hinshaw, F.T. Lee Jr., P.F. Laeseke, L.A. Sampson, C. Brace, Temperature isotherms during pulmonary cryoablation and their correlation with the zone of ablation, J. Vasc. Interv. Radiol. 21 (2010) 1424–1428.
[10] H.J. Hodgson, Primary hepatocellular carcinoma, Br. J. Hosp. Med. 29 (1983) (240, 246, 250 passim).
[11] Y. Koike, H. Yoshida, S. Shiina, T. Teratani, S. Obi, S. Sato, M. Akamatsu, R. Tateishi, T. Fujishima, Y. Hoshida, M. Kanda, T. Ishikawa, Y. Shiratori, M. Omata, Changes in hepatic functional reserve after percutaneous tumor ablation for hepatocellular carcinoma: long-term follow up for 227 consecutive patients with a single lesion, Hepatol. Int. 1 (2007) 295–301.
[12] D. Kopelman, Y. Kopelman, G. Spolianski, A. Zaretzki, L. Shechtman, M. Hashmonai, Thermal bile duct and duodenal protection during pancreatic cryoablation, Cryobiology 64 (2012) 235–239.
[13] P. Liang, Y. Wang, D. Zhang, X. Yu, Y. Gao, X. Ni, Ultrasound guided percutaneous microwave ablation for small renal cancer: initial experience, J. Urol. 180 (2008) 844–848 (discussion 848).
[14] P.J. Littrup, B. Jallad, V. Vorugu, G. Littrup, B. Currier, M. George, D. Herring, Lethal isotherms of cryoablation in a phantom study: effects of heat load, probe size, and number, J. Vasc. Interv. Radiol. 20 (2009) 1343–1351.
[15] N.J. Lygidakis, S.K. Sharma, P. Papastratis, V. Zivanovic, H. Kefalourous, M. Koshariya, I. Lintzeris, T. Porfiris, D. Koutsiouroumba, Microwave ablation in locally advanced pancreatic carcinoma – a new look, Hepatogastroenterology 54 (2007) 1305–1310.
[16] A. Mantovani, P. Allavena, A. Sica, F. Balkwill, Cancer-related inflammation, Nature 454 (2008) 436–444.
[17] K.K. Ng, C.M. Lam, R.T. Poon, T.W. Shek, J.Y. To, Y.H. Wo, D.W. Ho, S.T. Fan, Comparison of systemic responses of radiofrequency ablation, cryotherapy, and surgical resection in a porcine liver model, Ann. Surg. Oncol. 11 (2004) 650–657.
[18] S. Osada, H. Imai, H. Tomita, Y. Tokuyama, N. Okumura, N. Matsuhashi, F. Sakashita, K. Nonaka, Serum cytokine levels in response to hepatic cryoablation, J. Surg. Oncol. 95 (2007) 491–498.
[19] S. Permpongkosol, T.L. Nicol, R.E. Link, I. Varkarakis, H. Khurana, Q.J. Zhai, L.R. Kavoussi, S.B. Solomon, Differences in ablation size in porcine kidney, liver, and lung after cryoablation using the same ablation protocol, Am. J. Roentgenol. 188 (2007) 1028–1032.

[20] J.C. Rewcastle, G.A. Sandison, J.C. Saliken, B.J. Donnelly, J.G. McKinnon, Considerations during clinical operation of two commercially available cryomachines, J. Surg. Oncol. 71 (1999) 106–111.
[21] A. Rode, B. Bancel, P. Douek, M. Chevallier, V. Vilgrain, G. Picaud, L. Henry, F. Berger, T. Bizollon, J.L. Gaudin, C. Ducerf, Small nodule detection in cirrhotic livers: evaluation with US, spiral CT, and MRI and correlation with pathologic examination of explanted liver, J. Comput. Assist. Tomogr. 25 (2001) 327–336.
[22] M.S. Sabel, Cryo-immunology: a review of the literature and proposed mechanisms for stimulatory versus suppressive immune responses, Cryobiology 58 (2009) 1–11.
[23] A. Said, J. Wells, Management of hepatocellular carcinoma, Minerva. Med. 100 (2009) 51–68.
[24] A.J. Sheen, A.K. Siriwardena, The end of cryotherapy for the treatment of nonresectable hepatic tumors?, Ann Surg. Oncol. 12 (2005) 202–204.
[25] S.A. Shock, K. Meredith, T.F. Warner, L.A. Sampson, A.S. Wright, T.C. Winter 3rd, D.M. Mahvi, J.P. Fine, F.T. Lee Jr., Microwave ablation with loop antenna: in vivo porcine liver model, Radiology 231 (2004) 143–149.
[26] C.J. Simon, D.E. Dupuy, W.W. Mayo-Smith, Microwave ablation: principles and applications, Radiographics 25 (Suppl. 1) (2005) S69–83.
[27] C.J. Simon, D.E. Dupuy, D.A. Iannitti, D.S. Lu, N.C. Yu, B.I. Aswad, R.W. Busuttil, C. Lassman, Intraoperative triple antenna hepatic microwave ablation, Am. J. Roentgenol. 187 (2006) W333–W340.
[28] K.N. Tatsutani, J.D. Joye, R. Virmani, M.J. Taylor, In vitro evaluation of vascular endothelial and smooth muscle cell survival and apoptosis in response to hypothermia and freezing, Cryo. Lett. 26 (2005) 55–64.
[29] P.G. Thacker, M.R. Callstrom, T.B. Curry, J.N. Mandrekar, T.D. Atwell, M.P. Goetz, J. Rubin, Palliation of painful metastatic disease involving bone with imaging-guided treatment: comparison of patients' immediate response to radiofrequency ablation and cryoablation, Am. J. Roentgenol. 197 (2011) 510–515.
[30] H. Webb, M.G. Lubner, J.L. Hinshaw, Thermal ablation, Semin. Roentgenol. 46 (2011) 133–141.
[31] F.J. Wolf, D.J. Grand, J.T. Machan, T.A. Dipetrillo, W.W. Mayo-Smith, D.E. Dupuy, Microwave ablation of lung malignancies: effectiveness, CT findings, and safety in 50 patients, Radiology 247 (2008) 871–879.
[32] M.L. Woolley, D.A. Schulsinger, D.B. Durand, I.S. Zeltser, W.C. Waltzer, Effect of freezing parameters (freeze cycle and thaw process) on tissue destruction following renal cryoablation, J. Endourol. 16 (2002) 519–522.
[33] A.S. Wright, F.T. Lee Jr., D.M. Mahvi, Hepatic microwave ablation with multiple antennae results in synergistically larger zones of coagulation necrosis, Ann. Surg. Oncol. 10 (2003) 275–283.
[34] K.C. Xu, L.Z. Niu, W.B. He, Z.Q. Guo, Y.Z. Hu, J.S. Zuo, Percutaneous cryoablation in combination with ethanol injection for unresectable hepatocellular carcinoma, World J. Gastroenterol. 9 (2003) 2686–2689.
[35] K.C. Xu, L.Z. Niu, W.B. He, Y.Z. Hu, J.S. Zuo, Percutaneous cryosurgery for the treatment of hepatic colorectal metastases, World J. Gastroenterol. 14 (2008) 1430–1436.
[36] K.C. Xu, L.Z. Niu, Y.Z. Hu, W.B. He, Y.S. He, J.S. Zuo, Cryosurgery with combination of (125)iodine seed implantation for the treatment of locally advanced pancreatic cancer, J. Dig. Dis. 9 (2008) 32–40.
[37] K.C. Xu, L.Z. Niu, Y.Z. Hu, W.B. He, Y.S. He, Y.F. Li, J.S. Zuo, A pilot study on combination of cryosurgery and (125)iodine seed implantation for treatment of locally advanced pancreatic cancer, World J. Gastroenterol. 14 (2008) 1603–1611.
[38] Y. Yamauchi, Y. Izumi, M. Kawamura, S. Nakatsuka, H. Yashiro, N. Tsukada, M. Inoue, K. Asakura, H. Nomori, Percutaneous cryoablation of pulmonary metastases from colorectal cancer, PLoS One 6 (2011) e27086.